Influence of Gas Composition, Temperature and Pressure on Corona Discharge Characteristics

A. Bologa, H.-R. Paur, H. Seifert, and K. Woletz

Institute for Technical Chemistry, Karlsruhe Institute of Technology, Germany

Abstract—The tests were carried out with a high temperature / high pressure corona discharge ionizer in synthetic air, N_2, He and He-synthetic air and He-N_2 mixtures at gas pressure up to 2 MPa and gas temperature inside of the ionizer up to 500°C. The corona discharge onset voltage increases with increase of gas pressure. At constant applied voltage, the gas breakdowns take place at a lower pressure while for a higher pressure the corona discharge may not start yet. The negative corona currents are higher than for the positive corona. The corona onset and operation voltages increase linearly with increase of gas pressure. The stable corona discharge in He is observed at gas pressure up to $P = 10$ MPa. In helium the current-voltage characteristics can be approximated by a quadratic function. In the gas mixtures of ca. 50 Vol.% He in synthetic air or N_2, the stable corona discharge is observed at higher pressures comparative to pure synthetic air or N_2.

Keywords—Corona discharge, high pressure, high temperature, gas composition

I. INTRODUCTION

The use of corona discharge opens broad possibilities for various developments such as high temperature / high pressure electrostatic precipitators, electrohydrodynamic (EHD) pumps and thrusters, heat exchangers, ozone generation equipment, decomposition of toxic gases, etc. [1-4].

Corona discharge occurs when a high voltage (HV) is applied between the electrodes with substantially different radii of curvature. The high electric field in the vicinity of corona discharge electrode causes gas ionisation. The charge generation and transport in the gaseous media is one of the key-points of corona discharge. The net effect is that ions drift from the HV electrode to the grounded one. A space charge is formed and electric current flows between the electrodes.

The investigations of charge generation and transport phenomena in the corona discharge in the air were the object of various studies [3, 5-7]. Corona discharge in a point-plane electrode assembly as a function of gas pressure ($P < 10$ MPa) and point radius 1-20 μm was investigated in [6]. The transport coefficients and binary collision rates of electrons with neutrals in the air and its components were studied in [8]. The numerical modelling and simulation of corona discharge under different conditions was the topic of [3, 5, 9].

New fundamental questions appear with application of dense He gas [10-12] which is used as sample carrier gas in analytical techniques, filling gas for discharge tubes and lasers and purge gases in semiconductor industry. The use of helium at high temperature (up to 1000°C) and pressure (up to 10 MPa) opens perspectives for helium-cooled reactors [11, 13]. The use of He gas has a potential for high energy efficiency and faster control of gas flow in EHD gas pumping devices [14].

The experimental and analytical investigations of electrostatic and EHD phenomena in He gas were in the scope of various studies [15-19]. The current-voltage characteristics (CVC) of the corona discharge and charge transport in He were studied at various temperatures. It was shown that the mobility of charge carries in He strongly depends on gas pressure and purification, geometry of high-voltage electrodes and voltage polarity. Various forms of self-maintained discharge that arise in He at pressure $P = 0.1$-0.5 MPa are described in [20]. The CVCs and photocurrents of the He corona discharge under various flow conditions were investigated in [21]. The data about electrical and optical characteristics of a negative corona discharge in the electrode system "needle-grid" in a He/Xe/SF_6 mixture under the pressure $P = 100$-3000 kPa are presented in [22]. The fundamentals of the theory of corona discharge and main mechanisms of generation and disappearance of charge and excited particles are discussed for corona discharge in He in [23]. The direct current micro-plasma discharge in He at atmosphere pressure is simulated in [24]. The transport and Toundsen coefficients are presented for He in [25]. The measurements were carried out in small electrode gaps and for electrode system "sharp needle – plate".

In the current work authors discuss the results of the study of corona discharge CVCs in synthetic air, N_2, He and in gas mixtures such as He-synthetic air and He-N_2 at gas temperatures up to 500°C and pressures up to 2 MPa in an HT/HP ionizer.

II. INFLUENCE OF GEOMETRY OF HV ELECTRODE ON CORONA DISCHARGE CHARACTERISTICS

The corona ionizer consists of a grounded plate (thickness 3 mm) with $N = 3$ orifices (inner diameter $d_0 = 50$ mm). The metallic shells with height of are installed in the orifices (Fig. 1). Tests were carried out at atmospheric conditions with star-shaped disk HV

electrodes with $N_n = 3$; 5; 7 and 18 points and shells with height of $h_s = 5$; 10; 15 and 20 mm and electrode gap widths $L = 9$; 12 and 15 mm, correspondingly.

At constant electrode geometry, the decrease of electrode gap decreases corona discharge spark-over voltage U_{sp}. For the HV electrode with $N_n = 18$, by the tests without shells, the decrease of electrode gap from $L = 15$ mm to 9 mm decreased the U_{sp} from 19 kV to 12 kV. The spark-over current I_{sp} decreased from 1 mA to 0.7 mA. For constant value of the corona current $I_{op} = 0.6$ mA, the operation voltage was $U_{op} = 17$ kV for electrode gap $L = 15$ mm and $U_{op} = 10.5$ kV for $L = 9$ mm.

The use of grounded shells improves the stability of corona discharge CVCs, increases the operation current and minimizes the "edge effect". If the star-shaped electrodes are installed in the middle height of the grounded shells, the stable operation was observed for $h_s > L$. For example, for the ionizer with $N_n = 18$, $h_s = 20$ mm, $L = 9$ mm and $U_{op} = 10$ kV, the corona current increases from $I_{op} = 0.4$ mA for the ionizer without shells up to $I_{op} = 1.4$ mA with shells.

The corona current can be increased by increase of the number of high voltage electrodes in the ionizer or by increase of the number of sharp points per electrode. In experimentally tested ionizer, the increase of the number of sharp points per electrode from $N_n = 3$ to $N_n = 18$ increased the operation corona current (Fig. 1). For example, for $L = 9$ mm and $U_{op} = 11$ kV, the corona current increases from $I_{op} = 0.7$ up to $I_{op} = 1.8$ mA.

While at constant voltage the absolute value of corona current increases with increase of the number on sharp points N_n the mean corona current per single sharp point decreases [26]. For negative corona discharge and $U_{op} = 11$ kV the current per single point decreases from 0.08 mA for $N_n = 3$ to 0.033 mA for $N_n = 18$. The increase of the number of discharge points produces overlapping of corona fields at every point. The overlapped region markedly decreases concentration of the ions and corona current what, for example, for an electrostatic precipitator results in decrease of the overall precipitation efficiency [27]. For increasing of the mean corona current per sharp point it is necessary to increase the operation voltage.

For positive corona discharge, the current quickly increased with increase of applied voltage. The corona discharge in the ionizer was unstable and the spark-over discharges took place even at $U_{op} \sim 10$ kV. For the negative corona, the spark-over voltage was of $U_{sp} > 11$ kV and operation current was higher than for the positive corona discharge.

III. HIGH TEMPERATURE / HIGH PRESSURE TEST SET-UP

The test set-up for study of corona discharge current-voltage characteristics in dense gases includes a grounded high pressure vessel in which a HT/HP ionizer is installed (Fig. 2). The vessel is connected to a vacuum pump (Fa. Ilmvac GmbH, lower pressure 1 mbar). The HT/HP ionizer consists of a specially designed HV

insulator in which a HV support rod is installed [28]. The upper part of the HV support rod passes through the HV insulator and it is connected to the exit of a HV unit ($U_{max} = 20$ kV, $I_{max} = 10$ mA, DC negative/positive polarity, Fa. Heinzinger). On the bottom part of the HV support rod one or two star-shaped disk HV electrodes are installed [29]. By the experiments the electrode gap was 10 mm (tests with two HV electrodes) and 15 mm (tests with one HV electrode). The grounded tube electrode was equipped with a heating element which allowed heating of the grounded tube of the ionizer up to 500°C.

The test gas passed through the mass flow controller into the high pressure vessel. The gas from the vessel was 5 times evacuated before every measurement. The gas pressure inside of the vessel was changed from atmospheric up to 2.0 MPa. By the tests were measured the temperature of the grounded tube, the temperature of the wall of the high pressure vessel and the temperature of the top of the vessel where the high voltage insulator was installed. The direct (from on-set to break-down voltage) and in-direct (from break-down to on-set voltage) current-voltage characteristics were measured for positive and negative polarity corona discharge.
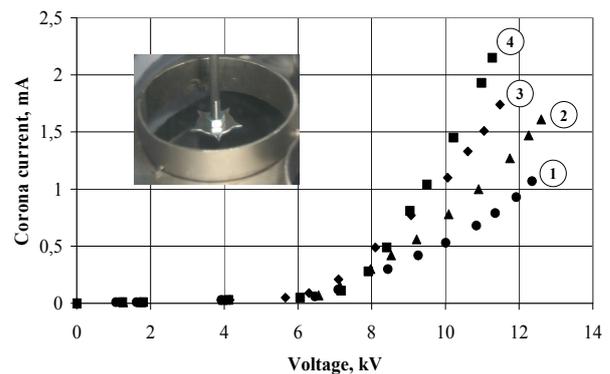

Fig.1. CVC for different number of points at star-shaped HV electrode: 1 – 3 points, 2 – 5 points, 3 – 7 points, 4 – 18 points.
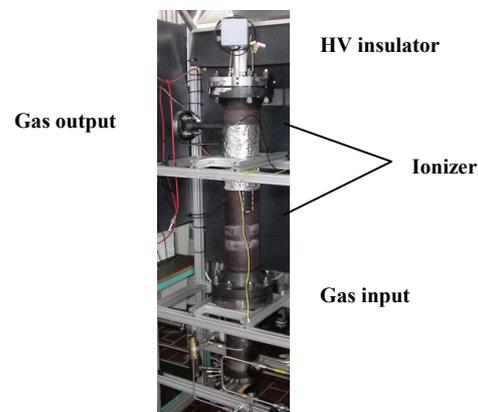

Fig.2. HT/HP vessel with a high voltage insulator.

IV. RESULTS

The corona discharge current-voltage characteristics (Fig. 3) were measured in synthetic air (79% N_2; 21% O_2). For positive polarity applied voltage, the corona current was suppressed at $P = 0.4$-0.5 MPa. For negative polarity applied voltage the suppression took place at $P =$ 0.6-0.7 MPa. The higher gas pressure results in lower ion mobility and narrows the drift region through which the ionic charge travels from the corona electrode to the grounded electrode. This takes place because the ionization coefficient per unit pressure diminishes. With increasing of the pressure the mean free path length diminishes and the collision frequency increases, thus reducing the ion mobility and resulting in a decrease of the corona current [21]. The increase of gas pressure increases the onset voltage of the corona discharge, increases the operation range of applied voltage and improves the stability of corona discharge.

At constant applied voltage, the gas breakdown took place at a lower pressure while for a higher pressure the corona discharge might not start yet.

The higher applied voltage requires higher space charge density in the air gap to keep the electric field on the corona electrode surface [7]. In order to have the same corona discharge current at high pressure, higher voltage needed to be applied. The increase of the corona discharge voltage can be described by the equation

$$U_{op} = aPL \frac{1}{\ln(PL)+b},\qquad (1)$$

here a and b are constants. For the air, the dependence of operation voltage from gas pressure can be approximated by a linear function $U_{op} = 30(PL)+1.35$ (kV).

At atmospheric conditions, the corona discharge in N_2 gas (Fig. 4) is more sensible for applied voltage as in the synthetic air.

In the corona discharge the He molecules are the dominating metastable component. The dominating charge carriers in the external region of the corona discharge are the molecular helium ions He_2^+ [31]. The corona discharge in helium strongly depends on gas purification. With better purification level, the mobility increased quickly and can reach electronic values [15].

The experimental study was carried out in He 4.6 gas (Table I). The CVCs were measured for gas pressure up to $P = 10$ MPa (Fig. 5).

One can see that for experimental conditions both negative and positive corona discharges are stable. For positive corona discharge the corona current is lower than for the negative corona discharge.

At atmospheric pressure the current of negative corona discharge in the He increases abruptly in the range of a few hundreds of volts. Possibly, this is due to the nature of the negative corona, whose charge carries, in the drift region, are electrons thus presenting a much higher mobility with respect to ions [21].

The CVCs in the helium can be approximated by a quadratic function. This is in a good agreement with [32]
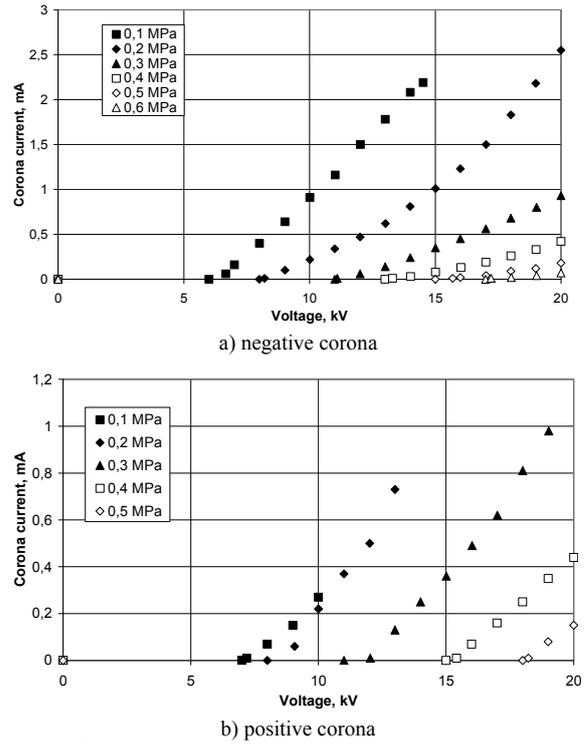

a) negative corona

b) positive corona

Fig.3. CVCs in synthetic air: room temperature conditions, $L = 10$ mm.
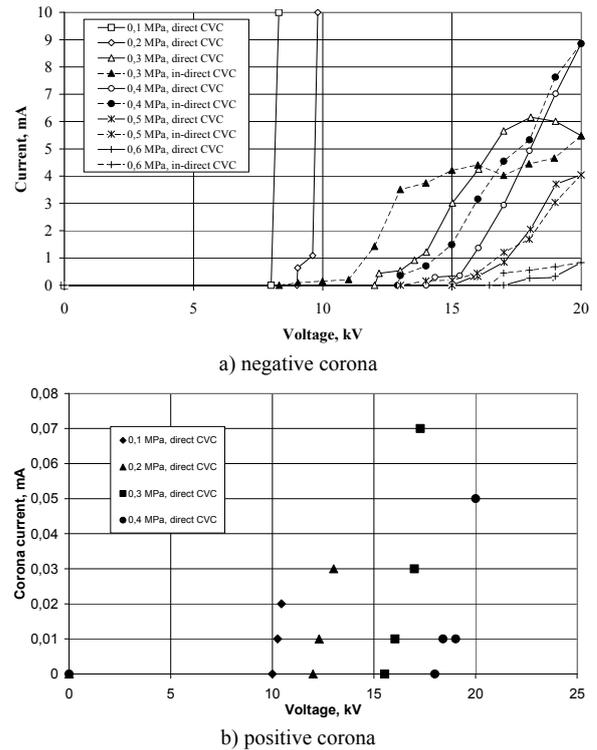

a) negative corona

b) positive corona

Fig.4. CVCs in N_2: room temperature conditions, $L = 10$ mm.

where the corona current in helium has also a quadratic function of the drift field. The operation voltage of the corona discharge increases with increase of gas density (Fig. 6). This dependence can be approximated with a linear function such $U_{op} = 0.1218(PL)+4.4436$ [kV]. So, the equation (1) can be used not only for calculation of
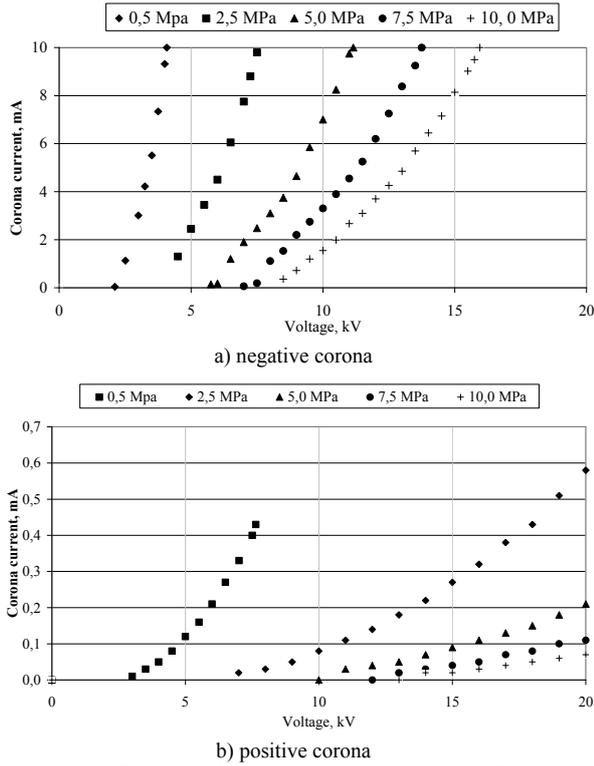
a) negative corona

b) positive corona

Fig.5. CVCs in He 4.6: atmospheric temperature, L = 15 mm.

TABLE I
He 4.6 COMPOSITION

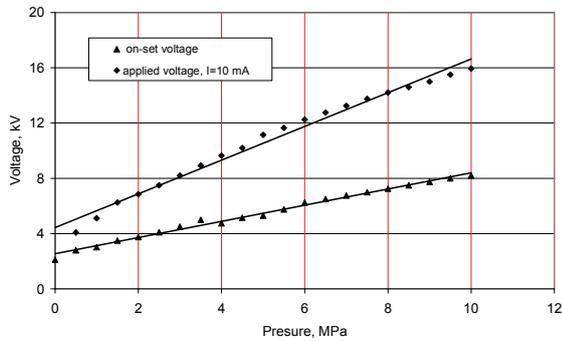| He Vol.%	N₂ ppm	O₂ ppm	CₓHᵧ ppm	CO,CO₂ ppm	H₂O ppm
≥99.996	< 10	<3	-	-	<3

Fig.6. Dependence of corona discharge on-set and applied voltage in the He 4.6 atmosphere pressure on gas pressure.

a) negative corona discharge

b) positive corona discharge

Fig. 7. CVCs of gas mixture: 10.01 Vol.% He in synthetic air.

a) negative corona

b) positive corona
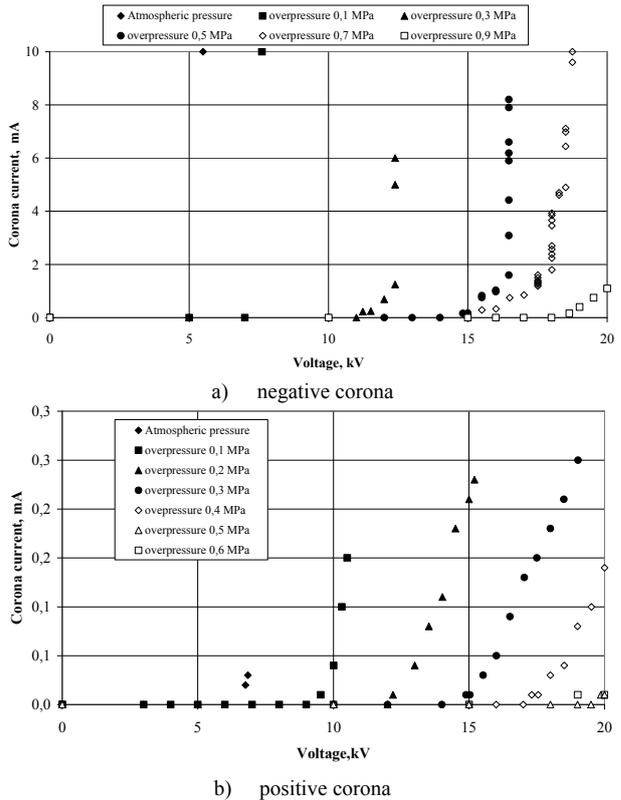
Fig. 8. Current-voltage characteristics of the gas: 9.94 Vol.% He in N₂.

the corona operation voltage in the air, but also in He atmosphere for different pressures and electrode gaps.

The tests were also carried out in gas mixtures such 10.01 and 49.21 Vol.% of He in synthetic air and 9.94 and 50.07 Vol.% of He in N₂ (Figs. 7-10). At constant applied voltage, the 10 Vol.% He in synthetic air increases the corona discharge operation current (Fig. 7).

The breakdown voltage increases gradually with increasing of the pressure. This can be attributed to the decrease in the ionisation cross-section when the electrons need more energy to break down the discharge gap. The increase of Vol.% concentration of He in the synthetic air changes the corona discharge parameters.
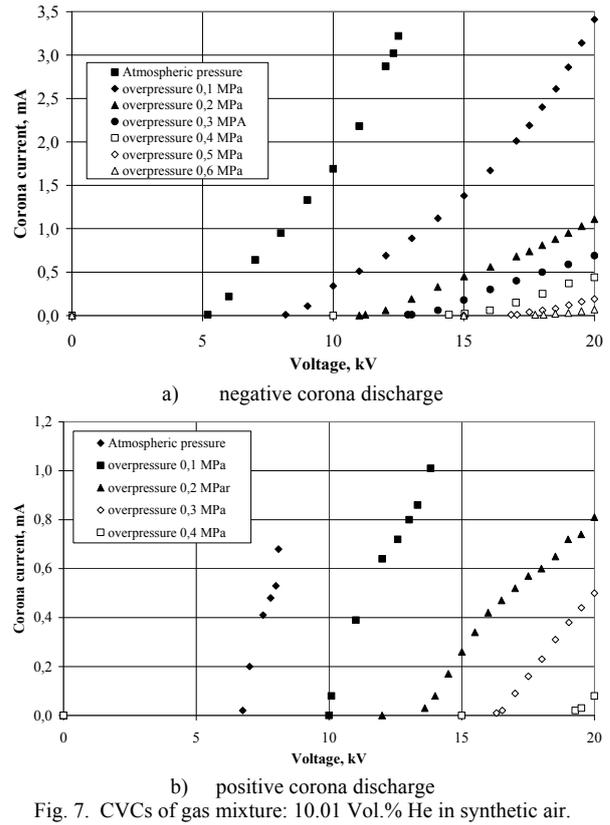
As higher is He concentration, as lower are the onset and breakdown voltages of the negative corona discharge at atmospheric conditions. At constant voltage, the increase of He Vol.% concentration increases the corona
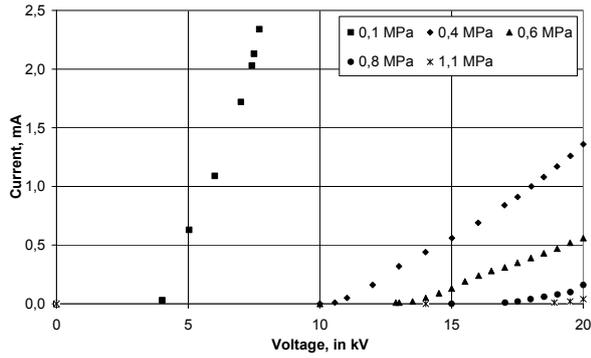
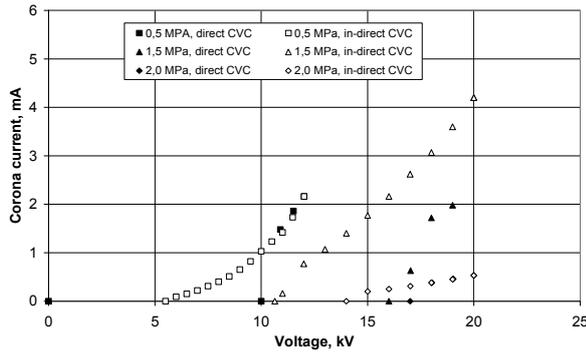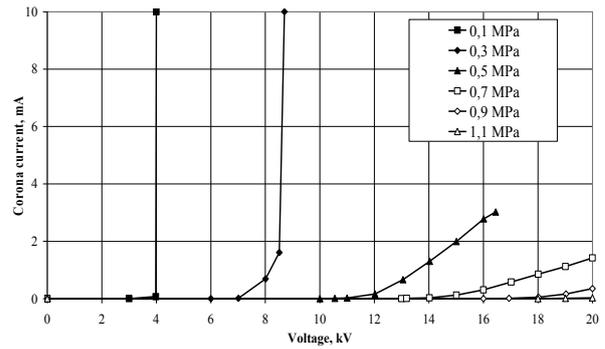Fig.9. Negative corona discharge CVCs in He-synthetic air: atmospheric temperature, He Vol.% 49.21, $L = 10$ mm.

Fig.10. Negative corona discharge CVCs in He-N_2 mixture: atmospheric temperature, He Vol.% 50.07, $L = 10$ mm.

a) negative corona

b) positive corona

Fig. 11. Corona discharge CVCs in synthetic air, $L = 10$ mm, $T = 500°C$.

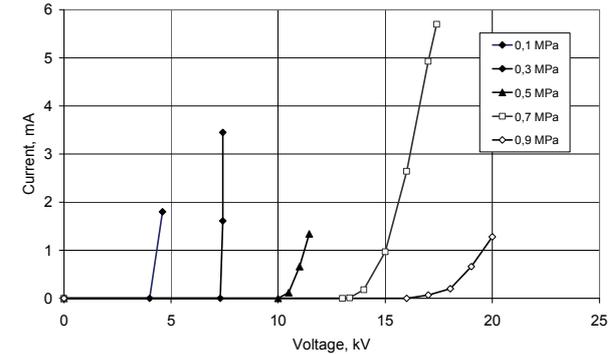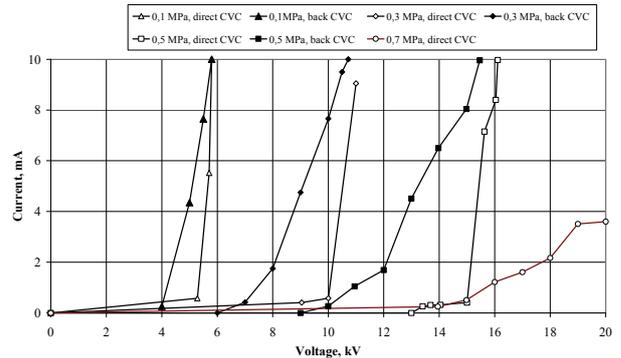Fig. 12. Negative corona discharge CVCs in N_2, $L = 10$ mm, $T = 500°C$.

discharge current. For $U_{op} = 20$ kV and over pressure $P = 0.3$ MPa, for 10 Vol.% of He in the synthetic air the operation current is $I_{op} = 0.75$ mA (Figs. 7 and 9) and for 49.21 Vol.% of He in synthetic air $I_{op} = 1.45$ mA.

With increase of Vol.% concentration of He in synthetic air, the concentration of O_2 molecules decreases. As the ionisation threshold energy of oxygen is much less if comparative with helium, the decrease of the concentration of O_2 molecules increases of the Townsend coefficient due to lowering of the inelastic collisions of electrons with O_2 molecules [25]. The decrease of inelastic collisions increases the number of fast electrons. This can be reason why at constant voltage, the increase of He Vol.% concentration in the synthetic air increases the corona current. The increase of helium concentration up to Vol.% 49.21 extends the range of gas pressure when the stable corona is observed. For negative corona the extend is up to $P = 1.1$ MPa and for positive corona the extend is up to $P = 0.6$ MPa, correspondingly (Figs. 7 and 9).

The introduction of He into the N_2 gas increases the stability of corona discharge with increase of pressure (Figs. 8 and 10). The difference between the on-set and break-down voltages increases in comparison with pure N_2. The corona current for positive corona is smaller than for negative one. In He-N_2 mixture (Fig. 10) the width of the hysteresis loop increases with increase of gas pressure. Such hysteresis of CVC-characteristics was also observed by [24] in "pins-mesh" electrodes in a unipolar corona discharge at different pressures of He/N_2 mixtures. The appearance of a hysteresis loop is explained by presence of a large amount of nitrogen

molecules in metastable electronic states in the studied plasma. The area of the observed hysteresis loop decreased with increase of the gas mixture pressure.

The CVCs of the corona discharge ionizer (electrode gap $L = 10$ mm) were measured at various gas pressures and temperatures. The results for the synthetic air at gas temperature $T = 500°C$ and different gas pressures are presented in the Fig. 11. The increase of gas temperature up to 500°C extends the values of gas pressures when the stable corona discharge takes place. The extension of gas pressure is up to $P = 1.1$ MPa for negative corona and up to $P = 0.9$ MPa for positive corona. The experimental results are in a good agreement with theory of gaseous discharge phenomena [1-3].

In nitrogen the negative corona discharge stabilises itself at gas pressure $P > 0.3$ MPa. The upper value of gas pressure is $P = 0.8$ MPa (Fig. 12). The positive corona discharge shows considerably lower currents
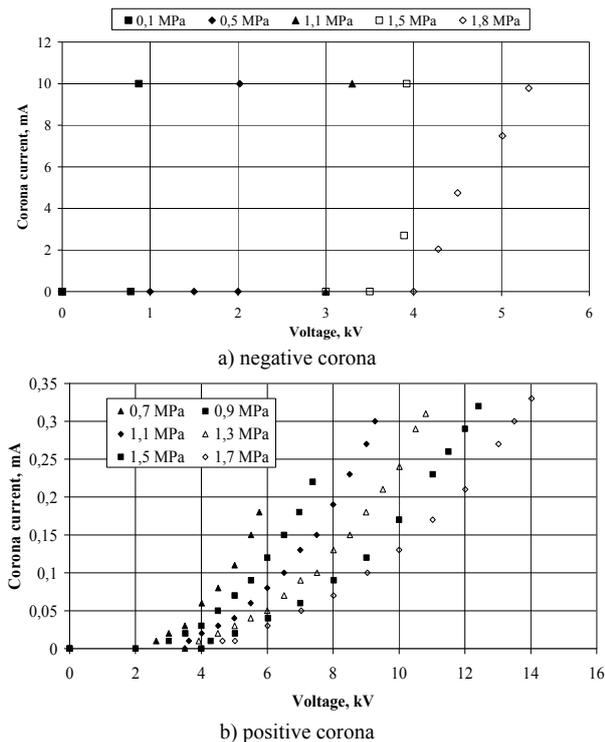
a) negative corona

b) positive corona
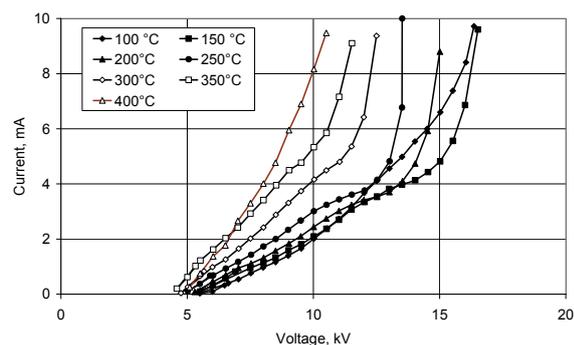Fig. 13. CVCs in He, L = 10 mm, T = 500°C.

Fig.14. Influence of gas temperature on negative corona discharge characteristics in He, $P \sim 2.0$ MPa.

comparative to negative corona. In hot gas and negative corona discharge, the hysteresis loop is more pronounced than at atmospheric conditions. The width of the loop increases with increase of gas pressure. Operation at in-direct CVC ensures stable corona discharge. At the same applied voltage, the in-direct CVCs show higher currents than the direct current-voltage characteristics.

In He the increase of gas temperature decreases the stability of negative corona discharge at pressures up to P = 1.6-1.7 MPa (Fig. 13 (a)). In the HT/HP ionizer stable negative corona discharge with currents I = 6-10 mA was observed at gas pressure P > 1.8 MPa. In comparison with gas temperature $T \sim 20$°C, where it was not possible to on-set stable positive corona discharge at high pressure, at T = 500°C the positive corona discharge was characterised by stable currents of I = 0.15-0.3 mA (Fig. 13 (b)). The increase of gas pressure at T = 500°C extends the gap between the values of on-set and break-down voltages.

The comparative curves for the negative corona CVCs for He at $P \sim 2.0$ MPa for different gas temperatures are presented in the Fig. 14. One can see that the increase of temperature slightly decreases corona on-set voltage. The gap between the on-set and break-down voltages narrows. With increase of temperature, the same corona current can be obtained at lower applied voltage.

V. CONCLUSIONS

The increase of gas pressure increases corona discharge onset and spark-over voltages. At constant applied voltage the increase of pressure decreases corona discharge current. At constant pressure, the negative corona discharge is characterized by higher currents than the positive corona discharge.

In He in the electrode gap of 10-15 mm it is possible to generate stable corona discharge at pressure up to P = 10 MPa. The increase of Vol.% concentration of He in the gas mixtures such as He-synthetic air and He-N_2 increases the critical value of gas pressure when the stable corona discharge is generated. The increase of temperature increases the gas pressure when stable corona discharge is observed.

In N_2 and He-N_2 at increased gas temperature, the hysteresis loop of the CVCs for the negative corona discharge is more pronounced than at atmospheric conditions. The loop width increases with increase of gas pressure.

REFERENCES

[1]   J. S. Chang, A. J. Kelly, and J. M. Crowley, *Handbook of Electrostatics Processes*, Marcel Dekker, New York, 1995.

[2]   I. Gallimberti, "Recent advancements in the physical modelling of electrostatic precipitators," *Journal of Electrostatics*, vol. 43, pp. 219-247, 1998.

[3]   J. Zhang, K. Adamiak, and G. S. P. Castle, "Numerical modeling of negative-corona discharge in oxygen under different pressures, " *Journal of Electrostatics*, vol. 65, pp. 174-181, 2007.

[4]   G. Rinard, D. E. Rugg, and T. Yamamoto, "High-temperature high-pressure electrostatic precipitator electrical characterization and collection efficiency," *IEEE Transactions on Industrial Applications,* vol. IA-23, pp. 114-119, 1987.

[5]   K. Adamiak and P. Atten, "Simulation of corona discharge in point-plane configuration," *Journal of Electrostatics*, vol. 61, pp. 85-98, 2004.

[6]   M. Haidara, A. Denat, and P. Atten, "Corona discharge in high pressure air," *Journal of Electrostatics*, vol. 40&41, pp. 61-66, 1997.

[7]   L. Zhao and K. Adamiak, "Numerical simulation of corona discharge in compressed gases with the effect of EHG flow," in *Proc. ESA Annual Meeting on Electrostatics*, Milwaukee, WI, 2008, Paper C2.

[8]   K. Masek, "Electron gas in discharge plasma in air," *Czechoslovak Journal of Physics,* vol. 34, pp. 655-664, 1984.

[9]   L. Zhao and and K. Adamiak, "EHD flow in air produced by electric corona discharge in pin-plate configuration," *Journal of Electrostatics*, vol. 63, pp. 337-350, 2005

[10] G. S. Filippov, R. G. Bogoyavlenskii, N. N. Ponomarev-Stepnoi, and A. O. Gol'tsev, "Modular high-temperature helium-cooled nuclear reactor with spherical fuel elements for electricity and hydrogen production," *Atomic energy,* vol. 96, pp.152-158, 2004.

[11] N. B. Vargaftik and N. Kh. Zimina, "Thermal conductivity of helium at temperatures of 0-1000°C and pressure of 1-200 Atm," *Atomnaya Energiya,* vol.19, pp. 300-303, 1965.

[12] J. E. Lovelock, "Method for purifying a continuous flow of helium and/or neon gas," USA Patent 4919690, December 17, 1987.

[13] A. G. Frank, S. Yu. Bogdanov, V. B. Burilina, N. P. Kyrie, and V. S. Markov, "Plasma Compression into a planar sheet under high-pressure He-filling," *Contributions to Plasma Physics*, vol. 40, pp. 106-112, 2000.

[14] J. S. Chang, H. Tsubone, Y. N. Chun, A. A. Berezin, and K. Urashima, "Mechanism of electrohydrodynamically induced flow in a wire-non-parallel plate electrode type gas pump," *Journal of Electrostatics*, vol. 67, pp. 335-339, 2009.

[15] N. Bonifaci, A. Denat, and B. Malraison, "Determination of charge mobility in He gas from current-voltage measurements in point-plane geometry," *IEEE Transactions on Industrial Applications*, vol. 37, pp. 1634-1640, 2001.

[16] A. K. Shuaibov, "The characteristics of a negative corona discharge in He/Xe/SF$_6$ mixture," *Czechoslovak Journal of Physics*, vol. 49, pp. 225-232, 1999.

[17] Q. Wang, I. Koleva, V. M. Donnely, and D. J. Economou, "Spatially resolved diagnostics of an atmospheric pressure direct current helium microplasma," *Journal of Physics D: Applied Physics,* vol. 38, pp. 1690-1697, 2005.

[18] J. Dutton, "A survey of electron swarm data," *Journal of Physical and Chemical Reference Data*, vol. 4, pp. 578-856, 1975.

[19] M. A. Hassouba, F. F. Elakshar, and A. A. Garamoon, "Measurements of the breakdown potentials for different cathode materials in the Townsend discharge," *Fizika A,* vol. 11, pp. 81-90, 2002.

[20] A. Z. Efendiev and A. A. Aliverdiev, "Multichannel helium discharge in a non-uniform field," *Dagestan State University, Izvestia Vysshikh Uchebnykh Zavedenii, Radiofizika*, vol. 20, pp. 1224-1231, 1977.

[21] R. Benocci and L. Mauri, "I-V characteristics and photocurrents of a He corona discharge under flow conditions," *Journal of Physics D: Applied Physics*, vol. 37, pp. 709-714, 2004.

[22] A. K. Shuaibov, L. L. Shimon, A. I. Minya, and A. I. Dashchenko, "Characteristics of negative corona discharge in the working media of atmospheric – pressure nitrogen lasers," *Journal of Applied Spectroscopy,* vol. 64, pp. 858-862, 1997.

[23] H. Sadat, N. Dubus, L. Pinard, J. M. Tatibouet, and J. Barrault, "Conduction heat transfer in a cylindrical dielectric barrier discharge reactor," *Applied Thermal Engineering,* vol. 29, pp. 1259-1263, 2009.

[24] Q. Wang, D. J. Economou, and V. M. Donnelly, "Simulation of a direct current microplasma discharge in helium at atmospheric pressure," *Journal of Applied Physics,* vol.100, 023301, 2006

[25] K. Masek, B. Kralikova, and J. Skala, "Experimental and numerical studies of the electron distribution function in He+O$_2$ dc discharge," *Czechoslovak Journal of Physics,* vol. B 30, pp. 885-896, 1980.

[26] J. Miller, B. Hoerer, and A. J. Schwab, "The impact of corona electrode configuration on electrostatic precipitator performance," *Journal of Electrostatics*, vol. 44, pp. 67-75, 1988.

[27] H. S. Surati, M. R. Beltran, and I. Raigorodsky, "Tubular electrostatic precipitators of two-stage design," *Environment International,* vol. 6, pp. 239-244, 1981.

[28] A Bologa, H. -R. Paur, and K. Woletz, "Influence of aerosol charging on real time measurement of particle number concentration downstream an electrostatic precipitator," presented at 2010 International Aerosol Conference, Helsinki, Finland, 2010.

[29] A. Bologa, H. -R. Paur, H. Seifert, and T. Wäscher, "Pilot-plant testing of a novel electrostatic collector for submicrometer particles," *IEEE Transactions on Industrial Applications*, vol. 41, pp. 882-890, 2005

[30] G. Rinard, D. E. Rugg, and T. Yamamoto, "High-temperature high-pressure electrostatic precipitator electrical characterization and collection efficiency," *IEEE Transactions on Industrial Applications,* vol. IA-23, pp. 114-119, 1987

[31] A. A. Belevtsev and L. M. Biberman, "On the theory of corona discharge," *Beiträge aus der Plasmaphysik,* vol. 23, pp. 313-330, 1983.

[32] M. Yasushi, S. Tochiyuki, and H. Yoshio, "Characteristics of discharge in a DC corona reactor for removing dilute SF$_6$," *IEEJ Transactions on Fundamentals & Materials*, vol. 126, pp. 328-334, 2006.